Diffusion of test particles in stochastic magnetic fields in the percolative regime

Marcus Neuer and Karl H. Spatschek
Institut für Theoretische Physik I, Heinrich-Heine-Universität Düsseldorf, D-40225 Düsseldorf, Germany
(Received 17 May 2006; published 12 September 2006)

For stochastic magnetic flux functions with percolative contours the test particle transport is investigated. The calculations make use of the stochastic Liouville approach. They start from the so-called *A*-Langevin equations, including stochastic magnetic field components and binary collisions. Using the decorrelation trajectory method, a relation between the Lagrangian velocity correlation function and the Eulerian magnetic field correlation is derived and introduced into the Green-Kubo formalism. Finite Larmor radius effects are included. Interesting results are presented in the percolation regime corresponding to high Kubo numbers. Previous results are found to be limiting cases for small Kubo numbers. For different percolative scenarios the diffusion is analyzed and strong influences of the percolative structures on the transport scaling are found. The finite Larmor radius effects are discussed in detail. Numerical simulations of the *A*-Langevin equation confirm the semianalytical predictions.

DOI: 10.1103/PhysRevE.74.036401 PACS number(s): 52.25.Fi, 05.40.−a, 52.25.Gj, 52.35.Ra

I. INTRODUCTION

Particle and heat transport phenomena are of major interest in several areas of modern physics. They appear with great diversity, e.g., in plasma and astrophysics [1]. In the basic concept of classical transport in magnetically confined plasmas, a magnetic field preferentially binds the particles along the field lines and reduces their ability to move in the perpendicular direction of the field. It is convenient to define test particle transport quantities, namely the mean square displacement and the diffusion coefficient, and to distinguish the transport in perpendicular and parallel directions. In the classical picture, large magnetic guiding fields reduce the perpendicular diffusion decisively. Collisions appear as an obstacle for the free motion along the field lines, on the one hand, and increase, on the other hand, the transport in the perpendicular direction. The specific reason for the extraordinary interest in the mechanisms of diffusion in stochastic fields lies in the unexpected large losses caused by anomalous transport [1]. The term anomalous refers to the strong deviation of the diffusion rate from the classical and neoclassical predictions [2]. Anomalous transport is caused by fluctuations of electric and magnetic fields [3]. To understand and control this type of transport is a major aim, e.g., with regard to the future designs of thermonuclear fusion reactors. Other important aspects are, e.g., the cosmic ray transport and magnetic field complexity in interstellar space.

In the physics of fusion plasmas there is also an additional motivation for the investigation of particle motion in stochastic fields. Auxiliary coils are being added to existing configurations to control transport in several tokamaks [4]. These additional coils are new and dominating sources of stochasticity. Examples can be found on the tokamaks Tore-Supra, DIII-D, and TEXTOR, and are being planned for JET and ASDEX-UPGRADE. The deterministic chaos of magnetic field lines produces a lot of important effects at the plasma boundary [5–7]. New methods [8] have been developed for a fast statistical analysis of transport in stochastic magnetic fields. Theories, e.g., Ref. [9], explain electron and positron runaway behaviors in stochastic fields.

Anomalous test particle transport theories start from stochastic Liouville-type models [10,11]. The vast majority is based on the *V*-Langevin equation in the guiding center limit. In fusion devices, the mean magnetic fields are sufficiently strong to support the small gyro-radii assumption over a broad area, at least for the electrons. The question remains in what way finite Larmor radii influence the transport, especially in regions where the guiding center assumption fails. Indeed, in tokamaks such areas can be found, e.g., in the vicinity of hyperbolic points. Our central intention is the description of these finite Larmor radius effects by analytical and numerical means.

The magnetic turbulence and related charged particle transport is also a long-standing problem in astrophysics. The rate of separation of magnetic lines of force in a random magnetic field was discussed [12,13]. Recently Ruffolo *et al.* [14] considered the separation of magnetic field lines in two-component turbulence. They showed that the separation of magnetic field lines follows an exponential law [13] when the slab component dominates the field line random walk. Chuychai *et al.* [15] discussed the suppressed diffusive escape of topologically trapped magnetic field lines. Particle transport in astrophysical plasmas with magnetic turbulence was investigated, e.g., by Qin *et al.* [16] who worked out perpendicular transport of charged particles in composite model turbulence. The basic investigations have many astrophysical applications, e.g., Refs. [17–20], explaining phenomena such as low-energy cosmic ray penetration into the heliosphere, the transport of galactic cosmic rays in and out of the interstellar magnetic field, the trapping of solar energetic particles by small scale topology, and the Fermi acceleration mechanism.

Galactic magnetic fields are parallel to the galactic disk and mostly aligned with the galactic spiral arms [21]. The typical Larmor radius of a cosmic ray particle in this field is several orders smaller than the height of the galactic disk in which most of the solar systems are located. In astrophysical plasmas of these dimensions, collisions are neglected and from the classical theory cosmic ray particles may be expected to remain very effectively trapped within the disk. Observations do not agree with this picture. Cosmic rays are

transported in perpendicular direction at several magnitudes higher than predicted by classical models. Obviously, a model based on entirely parallel magnetic fields aligned with the galactic arms is insufficient for a successful description of the cosmic rays. With a mean field in the parallel direction, there have to be additional perpendicular components that enable the particles to leave the galactic plasma. These components are induced by nonlinearities of the galactic field and can be regarded as stochastic. It is also an intention of this work to provide useful predictions of the diffusion that can be introduced into the models of cosmic rays. Magnetic fields occurring in the galaxy consist of small guiding fields. Then it is required to include the complete gyrational motion.

Another aspect of the transport in stochastic magnetic fields concerns the structure of the perturbation field. Magnetic perturbations can be regarded to be generated from a stochastic flux function. In some cases that are related to Kubo numbers greater than 1 the flux function gets percolative contours [22]. In such cases the field lines are forced to move around the contour lines. This can lead to the very interesting fact that a certain number of field lines is trapped within the percolative map of the flux function and can no longer contribute to transport. When field lines become trapped within areas of the magnetic flux, the so-called flux tubes [17], the transport is changed significantly [23–29]. The low-frequency percolation scaling for particle diffusion in electrostatic turbulence has been discussed by Reuss and Misguich [30].

A method used in connection with percolative systems is the decorrelation trajectory method (DCT), developed by Vlad *et al.* in Ref. [26]. In the present paper we apply the DCT to the problem of test particle transport in systems with finite Kubo numbers. The Kubo number is defined as the ratio of the distance a particle travels during an autocorrelation-time over the correlation distance. For small Kubo numbers, the so-called Corrsin approximation [31] turns out to be applicable. The central problem is the relation between Lagrangian and Eulerian correlation functions [32,33] for all Kubo numbers. To further develop the theory in the percolation regime on the basis of stochastic differential equations, a consequent comparison between the Corrsin approximation and the DCT is needed. It is a central intention of the present work to provide an analytical relation between the Corrsin correlation functions and the DCT correlation functions, as well as an in depth investigation of the combined effects of percolation structures and finite Larmor radii.

The paper is organized as follows. In Sec. II we introduce the *A*-Langevin model and present the general formulation for the velocity correlation function. The latter includes finite Larmor radius effects. The Green-Kubo formalism is used to derive a differential equation for the diffusion coefficient and the mean-squared displacement (MSD). Section III makes use of the decorrelation trajectory method (DCT) to determine the Lagrangian correlation function. Equations for the running diffusion coefficient are derived. Additionally, a relation between the Corrsin approximation and the DCT is discussed. Previous results within the Corrsin approximation [32,34] turn out to be limiting cases of the more general DCT treatment.

The main results of the present work are shown in Sec. IV. The influence of finite Larmor radii is pointed out for a broad range of Kubo numbers and different states of collisionality. The existence of a regime with decisively higher transport than in common guiding center theories is demonstrated. The results are verified by numerical simulations for the *A*-Langevin equation.

The work is concluded by a short summary and discussion in Sec. V. Details of our calculations are placed into three appendixes.

II. *A*-LANGEVIN APPROACH

We start with a magnetic field of the form $\mathbf{B}=B_0(b_0\mathbf{e_z}+b_x\mathbf{e_x}+b_y\mathbf{e_y}+b_z\mathbf{e_z})$, composed of a guiding field B_0b_0 in the z direction (parallel component) and perturbations in x, y (perpendicular components), and z directions. The factor B_0 takes care of the dimension of the magnetic field. With the assumption of two-dimensional perturbations, we restrict our investigation to situations corresponding to relatively strong guiding fields, that means for any parallel perturbation b_z we assume that $|b_0|\geqslant|b_z|,|b_x|,|b_y|$. Under such circumstances the influence of b_z can be neglected. We define the gyrofrequency unit $\Omega=ZeB_0/mc$, where m is the test particle (electron or ion) mass and Ze is the test particle charge. Note that with this definition the typical Larmor frequency is given by $\Omega_L=\Omega b_0$. The Larmor radius is defined as $\rho_L=v_{th}/(\Omega b_0+\Omega\beta)$, where the thermal velocity v_{th} and the relative strength β of the magnetic perturbations have been introduced.

The *A*-Langevin equation is the equation of motion for a test particle experiencing the effect of the magnetic field (including its stochastic contribution) and random collisions (through $\mathbf{a}$). A friction parameter ν models the average effect of these collisions,

$$\frac{d}{dt}\mathbf{u}=\frac{Ze}{mc}\mathbf{u}\times\mathbf{B}-\nu\mathbf{u}+\mathbf{a}. \tag{1}$$

Integration of $\mathbf{u}(t)$ leads to the trajectory of the particle, $\mathbf{R}(t)=\int_0^t\mathbf{u}(t')dt'$. We apply a white noise correlation spectrum for the collisions, with $\langle\mathbf{a}\rangle=\mathbf{0}$ and $\langle a_i(t_1)a_j(t_2)\rangle=A\delta_{ij}\delta(t_1-t_2)$.

It has already been shown in Ref. [34] that an explicit solution of Eq. (1) can be written in terms of $\boldsymbol{\eta}$,

$$\langle\boldsymbol{\eta}_\perp(t+\tau)\boldsymbol{\eta}_\perp(t)\rangle_\perp=\frac{v_{th}^2}{2}\exp(-\nu\tau)\cos(\Omega b_0\tau), \tag{2}$$

$$\langle\eta_\parallel(t+\tau)\eta_\parallel(t)\rangle_\parallel=\frac{v_{th}^2}{2}\exp(-\nu\tau). \tag{3}$$

The velocity $\boldsymbol{\eta}$ is the solution without a stochastic magnetic field corresponding to the classical transport situation.

The transport of test particles can be deduced from the velocity correlation function. Once the Lagrangian velocity correlation is known, the mean square displacement (MSD) and the diffusion coefficient are typically obtained from the Green-Kubo formula

$$\frac{d^2}{dt^2}\langle \delta r_i^2 \rangle = 2\frac{d}{dt}D(t) = \langle\langle\langle u_i(t_1)u_i(t_2)\rangle_{\mathbf{b}}\rangle_{\perp}\rangle_{\parallel}, \quad i = x,y,z. \tag{4}$$

The Green-Kubo formula connects the MSD, respectively the running diffusion coefficient $D(t)$, with the velocity correlation function. It should be solved with the initial conditions $D(0)=0$ and $\langle \delta r_i^2(0)\rangle = 0$. The perpendicular velocity correlation has been discussed in Ref. [34]. We call the contribution from the magnetic perturbation terms the anomalous contribution, thereby distinguishing between classical transport and the anomalous transport,

$$u_x(t_1)u_x(t_2) = [\eta_x(t_1)\eta_x(t_2)]^{CL} + [u_x(t_1)u_x(t_2)]^{AN}. \tag{5}$$

The velocity correlation functions still require averaging with respect to the stochastic variables. A rigorous perturbation theory for strong guiding fields leads to

$$\langle u_x(t_1)u_x(t_2)\rangle_{\mathbf{b},\perp,\parallel}^{AN} \equiv L^{(0)} + L^{(1)}, \tag{6}$$

with the correlation functions

$$L^{(0)} = \frac{1}{b_0^2}\langle \eta_z(t_1)\eta_z(t_2)\langle\langle b_y[\mathbf{x}(t_1)]b_y[\mathbf{x}(t_2)]\rangle_{\mathbf{b}}\rangle_{\perp}\rangle_{\parallel}, \tag{7}$$

$$L^{(1)} = \frac{\rho_L^2}{v_t^2 b_0^2}\langle \eta_z(t_1)\eta_z(t_2)\langle\langle b_y'[\mathbf{x}(t_1)]b_y'[\mathbf{x}(t_2)]\rangle_{\mathbf{b}}\rangle_{\perp}\rangle_{\parallel}. \tag{8}$$

We refer to $L^{(0)}$ as the guiding center limit. It represents the zeroth order of the perturbation theory. $L^{(1)}$ is the first order and contains the effects of finite Larmor radii, as can be seen from the right-hand side of Eq. (8).

A central question concerns the averages of magnetic field components. The magnetic correlation is given in Eulerian coordinates and has thus to be transformed to Lagrangian coordinates. Such a problem exists in practically all applications of turbulence and transport theory [33]. Typically, an approximation due to Corrsin [31] is applied which provides a straightforward estimation for the Lagrangian correlation function. Unfortunately, this rather simple technique goes along with a strong restriction on the stochastic regime defined in terms of the dimensionless magnetic Kubo number $\kappa = \frac{\beta\lambda_{\parallel}}{b_0\lambda_{\perp}}$. Here we introduced the perpendicular and parallel correlation lengths $\lambda_{\perp}$ and $\lambda_{\parallel}$. When using the Corrsin approximation [34] we found very good agreement of our model equations with simulations of the system (1) for small Kubo numbers. Our intention is now to extend the model to the complete range of Kubo numbers. An alternative method has to be applied in order to cover a broader range of Kubo numbers. The investigation will include the Corrsin approximated results as a limiting case for small Kubo numbers.

III. DCT METHOD

In a series of papers Vlad and co-workers [26–29] developed a new procedure for the Lagrangian correlation functions, called the decorrelation trajectory method. It was designed for large Kubo numbers and can be regarded as a substitute for the Corrsin approximation. The method has been used within the guiding center approximation (when the so-called *V*-Langevin equation applies). Here, we shall adapt the DCT to the more general problem of the correlation functions of the *A*-Langevin equation. The perturbation field $\mathbf{b}$ is assumed to have only a two-dimensional structure. This condition is fulfilled for finite but small Larmor radii. The stochastic field $\mathbf{b}$ is generated by the scalar magnetic potential $\phi(\mathbf{x},z)$,

$$\mathbf{b}(\mathbf{x},z) = \nabla\phi(\mathbf{x},z) \times \mathbf{e}_z, \tag{9}$$

which we will call the flux function. The stochastic properties of this function are presented in Appendix A. The vector $\mathbf{x}=(x,y)$ refers to the perpendicular coordinates, whereas z can be regarded as the parallel coordinate. Magnetic field lines follow from the flux function by the relation $d\mathbf{x}/dz = \mathbf{b}$. Within the DCT formulation we have

$$L_{\mathrm{DCT}}^{(0)} = \frac{1}{b_0^2}\int_{-\infty}^{\infty} P(\eta^0)P(\mathbf{b}^0)P(\phi^0)\eta^0 b_y^0 \times \langle\langle \eta_z(t)b_y[\mathbf{x}(t),z(t),t]\rangle_S\rangle_{\perp} d\eta_z^0 d\mathbf{b}^0 d\phi^0, \tag{10}$$

and

$$L_{\mathrm{DCT}}^{(1)} = \left\langle \frac{\rho_L^2}{v_t^2 b_0^2}\int_{-\infty}^{\infty} P(\eta_x^0)P(\eta_y^0)P(\eta_z^0)P(\mathbf{b}'^0)P(\phi^0) \times \eta^0 b_y'^0 \langle \eta_z(t)b_y'[\mathbf{x}(t),z(t),t]\rangle_S \times d\eta_x^0 d\eta_y^0 d\eta_z^0 d\mathbf{b}'^0 d\phi^0 \right\rangle_{\perp}. \tag{11}$$

Equations (10) and (11) are still exact since so far no approximation has been applied. Next, we assume Gaussian probabilities $P(x)$. We do not know the trajectory $\mathbf{r}=(\mathbf{x},z)$. But the subensemble decomposition leads to a significant advantage: For each subensemble the values of ϕ^0, η^0, and $\mathbf{b}^0$ are fixed. Within the DCT subensemble we can determine each trajectory for a mean field $\langle \mathbf{b}(\mathbf{x},z)\rangle_S$ by solving the *A*-Langevin equation. The crucial simplification of that technique is that all contributions from the magnetic field are now nonstochastic values. The fictitious trajectory, along which a particle would travel if it is introduced into the subensemble magnetic mean field, is called the decorrelation trajectory.

The major approximation of the DCT [26] allowing the transition from the Eulerian to the Lagrangian expression, is to evaluate the formulas (10) or (11) by substituting for the unknown trajectory $\mathbf{x}(t)$ the decorrelation trajectory. This trajectory is introduced into the expression for the averaged field $\langle \mathbf{b}(\mathbf{x}=\mathbf{X},z)\rangle_S$. With the trajectory $X(t)$ given by the *A*-Langevin equation, Eqs. (10) and (11) determine the Lagrangian velocity correlator. The first task is then to find the average $\langle \mathbf{b}(\mathbf{x},z)\rangle_S$ in each subensemble defined by $\mathbf{b}^0$ and ϕ^0. Additionally, we need expressions for the averages occurring in the DCT equations.

The decorrelation trajectory itself is given by an *A*-Langevin equation

$$\ddot{\mathbf{X}}(t) = \dot{\mathbf{U}}(t) = \frac{Ze}{mc}\mathbf{U}(t)\{B_0[b_0\mathbf{e}_z + \langle \mathbf{b}(\mathbf{X},z)\rangle_S]\} - \nu\mathbf{U}(t) + \mathbf{a}(t), \tag{12}$$

containing the nonstochastic subensemble average $\langle \mathbf{b}(\mathbf{x},z)\rangle_S$. The collisions **a** are still stochastic entries. Each subensemble produces an averaged **b** field. One can calculate this average by using the conditional probability to find (within the subensemble defined by ϕ^0 and $\mathbf{b}^0$) a field **b** at the position **x**,

$$\langle \mathbf{b}(\mathbf{x},z)\rangle_S = \int_{-\infty}^{\infty} d\mathbf{b}\mathbf{b}P(\mathbf{b},\mathbf{x}|\phi^0\mathbf{b}^0), \tag{13}$$

where one uses

$$P(\mathbf{b},\mathbf{x}|\phi^0\mathbf{b}^0) = \frac{\langle \delta(\mathbf{b}-\mathbf{b}(\mathbf{x},z,t))\,\delta(\phi^0-\phi(\mathbf{0}))\,\delta(\mathbf{b}^0-\mathbf{b}(\mathbf{0}))\rangle_S}{\langle \delta(\phi^0-\phi(\mathbf{0}))\,\delta(\mathbf{b}^0-\mathbf{b}(\mathbf{0}))\rangle_S}. \tag{14}$$

With the conditional probability we immediately find

$$\langle \mathbf{b}(x,y)\rangle_S = \begin{pmatrix} b_x^0\mathcal{E}_{xx} + b_y^0\mathcal{E}_{xy} + \phi^0\mathcal{E}_{\phi x} \\ b_x^0\mathcal{E}_{yx} + b_y^0\mathcal{E}_{yy} + \phi^0\mathcal{E}_{\phi y} \end{pmatrix} = \begin{pmatrix} -\frac{\beta^2}{\lambda_\perp^2}\{y\lambda_\perp^2\phi^0 + (y^2-\lambda_\perp^2)b_x^0 - xyb_y^0\}e^{-\Theta(\mathbf{x},z)} \\ \frac{\beta^2}{\lambda_\perp^2}\{x\lambda_\perp^2\phi^0 + xyb_x^0 + (\lambda_\perp^2-x^2)b_y^0\}e^{-\Theta(\mathbf{x},z)} \end{pmatrix}. \tag{15}$$

We split the y component into x and z dependencies defining

$$\frac{\beta^2}{\lambda_\perp^2}\{x\lambda_\perp^2\phi^0 + xyb_x^0 + (\lambda_\perp^2-x^2)b_y^0\}e^{-\Theta(\mathbf{x},0)}e^{-\Theta(0,z)} \equiv F_\perp(\mathbf{x})F_\parallel(z). \tag{16}$$

In the analysis of the DCT terms, we will only need the y component of $\langle \mathbf{b}(\mathbf{x},y)\rangle_S$.

Summarizing, we can derive a subensemble decomposition of the Eulerian correlation function for both the magnetic field and for the velocity of a particle, depending on the averaged **b** field in each subensemble. The average, $\langle \mathbf{b}(\mathbf{x},y)\rangle_S$, is given as a function of **x** and z.

A similar result is obtained for the averaged derivative in the subensemble,

$$\langle \mathbf{b}'(x,y)\rangle_S = \begin{pmatrix} b_x'^0\bar{\mathcal{E}}_{x'x'} + b_y'^0\bar{\mathcal{E}}_{x'y'} \\ b_x'^0\bar{\mathcal{E}}_{y'x'} + b_y'^0\bar{\mathcal{E}}_{y'y'} \end{pmatrix}. \tag{17}$$

Note that the ϕ^0 part vanishes.

Using the definitions of the derivative correlations of Appendix A we immediately find for the x component

$$\langle b_x'(x,y)\rangle_S = \{T_1(\mathbf{x})\eta_x^0\eta_x(t) + T_2(\mathbf{x})\eta_y^0\eta_y(t) + T_3(\mathbf{x})\eta_z^0\eta_z(t)\}e^{-z^2/2\lambda_\parallel^2}, \tag{18}$$

with the abbreviations

$$T_1(\mathbf{x},\lambda_\perp) = \left(\frac{x^2y^2\beta^2b_x'^0}{\lambda_\perp^6} - \frac{x^2\beta^2b_x'^0}{\lambda_\perp^4} - \frac{y^2\beta^2b_x'^0}{\lambda_\perp^4} + \frac{\beta^2b_x'^0}{\lambda_\perp^2} - \frac{x^3y\beta^2b_y'^0}{\lambda_\perp^6} + \frac{3xy\beta^2b_y'^0}{\lambda_\perp^4}\right)e^{-x^2/2\lambda_\perp^2 - y^2/2\lambda_\perp^2}, \tag{19}$$

$$T_2(\mathbf{x},\lambda_\perp) = \left(\frac{y^4\beta^2b_x'^0}{\lambda_\perp^6} - \frac{6y^2\beta^2b_x'^0}{\lambda_\perp^4} + \frac{3\beta^2b_x'^0}{\lambda_\perp^2} - \frac{xy^3\beta^2b_y'^0}{\lambda_\perp^6} + \frac{3xy\beta^2b_y'^0}{\lambda_\perp^4}\right)e^{-x^2/2\lambda_\perp^2 - y^2/2\lambda_\perp^2}, \tag{20}$$

$$T_3(\mathbf{x},\lambda_\perp) = \left(\frac{\beta^2b_x'^0}{\lambda_\parallel^2} - \frac{z^2\beta^2b_x'^0}{\lambda_\parallel^4} - \frac{y^2\beta^2b_x'^0}{\lambda_\parallel^2\lambda_\perp^2} + \frac{y^2z^2\beta^2b_x'^0}{\lambda_\parallel^4\lambda_\perp^2} + \frac{xy\beta^2b_y'^0}{\lambda_\parallel^2\lambda_\perp^2} - \frac{xyz^2\beta^2b_y'^0}{\lambda_\parallel^4\lambda_\perp^2}\right)e^{-x^2/2\lambda_\perp^2 - y^2/2\lambda_\perp^2}. \tag{21}$$

The Kubo number enters the Lagrangian correlation function implicitly through the DCT. The solution of Eq. (12) may show trapping. Depending on the autocorrelation time, the total distance traveled during the autocorrelation time may become large compared to the (perpendicular) correlation length. That situation corresponds to large Kubo numbers.

A. Zeroth order Lagrangian correlation function

We use the coordinate transformation [32] $\mathbf{x}(\mathbf{t}) \to \mathbf{x}(\mathbf{t}) + \xi$ and define $\xi = (\xi_\mathbf{x}, \xi_\mathbf{y})$ being responsible for all perpendicular deviations from the trajectory. With this definition an arbitrary Eulerian correlation function $\mathcal{E}$ can be calculated by

$$\langle \mathcal{E}(x,z)\rangle_\perp = \int_{-\infty}^{\infty} \mathcal{E}(x+\xi_x)\langle \delta[\xi_x - \xi_x(t)]\rangle_\perp d\xi_x. \tag{22}$$

This formulation is similar to the relation derived within the Corrsin approximation. Using the Fourier representation of the δ function we can easily find

$$P(\xi_x) \equiv \langle \delta[\xi_x - \xi_x(t)]\rangle_\perp = \frac{1}{\sqrt{2\pi\langle \xi^2(t)\rangle}}\exp\left(-\frac{\xi_x^2}{2\langle \xi^2(t)\rangle_\perp}\right), \tag{23}$$

i.e., a Gaussian distribution in ξ_x which we will denote with the symbol $P(\xi_x)$. Because of symmetry reasons we have also $\langle \xi_x^2\rangle = \langle \xi_y^2\rangle \equiv \langle \xi^2(t)\rangle$. For the zeroth order we can apply the average at the very beginning of the calculation, namely on the Eulerian correlator,

$$\langle A(\mathbf{x},z;\lambda_\perp)\rangle_\perp = \int_{-\infty}^{\infty}\int_{-\infty}^{\infty} \beta^2\lambda_\perp^2 \exp\left[-\frac{(x+\xi_x)^2 + (y+\xi_y)^2}{2\lambda_\perp^2} - \frac{z^2}{2\lambda_\parallel^2}\right] \times P(\xi_x)P(\xi_y)d\xi_x d\xi_y, \tag{24}$$

leading the averaged Eulerian correlation in the form

$$\langle A(\mathbf{x},z;\lambda_\perp)\rangle_\perp = \mathcal{N}A[\mathbf{x},z;\lambda_\perp + \langle\xi^2(t)\rangle], \tag{25}$$

where

$$\mathcal{N} = \left(1 + \frac{\xi^2(t)}{\lambda_\perp^2}\right)^{-1}. \tag{26}$$

This finally leads to

$$Z \equiv \langle\langle\langle \eta_\parallel(t) b_y[\mathbf{x}(t),z(t),t]\rangle_S\rangle_\parallel\rangle_\perp = \mathcal{N}F_\perp[\mathbf{x};\lambda_\perp + \langle\xi^2(t)\rangle]\int_{-\infty}^{\infty} F_\parallel(z)M_\parallel(z)dz. \tag{27}$$

Note the appearance of the Corrsin term $\mathcal{N}$, which does not depend on the DCT. Within this picture the decorrelation trajectory itself appears only in the perpendicular coordinates x and y. The definition of $M_\parallel$ is given in Appendix B. The further integration can also be performed directly; it is later not affected by any assumption on the trajectory. The z integration can be carried out, using the expression for $M_\parallel(z)$,

$$Z = F_\perp[\mathbf{x},\lambda_\perp + \langle\xi^2(t)\rangle] \times \mathcal{N}\left(\eta^0\mathcal{M}\chi_\parallel \nu e^{-\nu t} - \frac{\eta^0\varphi_\parallel^2[1-\chi_\parallel\nu e^{-\nu t}]}{\lambda_\parallel^2}\mathcal{M}^3\right) \times e^{-[\langle z(t)\rangle_S^2/2\lambda_\parallel^2]\mathcal{M}^2}. \tag{28}$$

This average can now be introduced into the DCT integrations, yielding the result

$$L_{\mathrm{DCT}}^{(0)} = \mathcal{S}_0(t)\mathcal{N}\mathcal{M}\left(\chi_\parallel\nu e^{-\nu t} + \mathcal{M}^2(\chi_\parallel\nu e^{-\nu t} - 1)\frac{\varphi_\parallel^2}{\lambda_\parallel^2}\right).$$

We introduced a function $\mathcal{S}_0(t)$ which contains the information on the percolation map,

$$\mathcal{S}_0(t) = \frac{1}{(1+\mathcal{M}^2\varphi^2/\lambda_\parallel^2)^{3/2}}\int_{-\infty}^{\infty}\int_{-\infty}^{\infty}\int_{-\infty}^{\infty} b_y^0 F_\perp[\mathbf{X};\lambda_\perp + \langle\xi^2(t)\rangle] \times P(b,\phi)db_x^0db_y^0d\phi^0. \tag{29}$$

Although the function $\mathcal{S}_0(t)$ is quite complicated, and therefore typically evaluated numerically, we can still find interesting analytical properties: $\lim_{\lambda_\perp\to\infty}\mathcal{S}_0(t)=1$ as well as $\lim_{\lambda_\perp\to 0}\mathcal{S}_0(t)=0$. This can be checked easily by inserting Eq. (16) into Eq. (29). An obvious connection between both methods, the DCT and the Corrsin approximation, can be identified by

$$\lim_{\kappa\to 0} L_{\mathrm{DCT}}^{(0)} = L_{\mathrm{Corrsin}}^{(0)}, \tag{30}$$

where $L_{\mathrm{Corrsin}}^{(0)}$ corresponds to the results [34] for the A-Langevin equation within the Corrsin approximation. The latter was restricted to small Kubo numbers and is recovered here in a more general context.

As stated already, the validity of the Corrsin approximation is restricted to small Kubo numbers. Evaluations of many simulations showed that $\kappa \leqslant 0.1$ can be considered as the regime where the Corrsin approximation leads to qualitatively correct, and quantitatively acceptable, results.

B. First order Lagrangian correlation function

The evaluation of the first order correction term (8) within the DCT subensembles (11) is significantly more involved, but in principle similar to the previous case. We have

$$L_{\mathrm{DCT}}^{(1)} = \frac{\rho_L^2}{v_t^2 b_0^2}\Bigg\langle \int_{-\infty}^{\infty} P(\eta_x^0)P(\eta_y^0)P(\eta_z^0)P(\mathbf{b}'^0)P(\phi^0) \times \eta_z^0 b_x'^0 \int_{-\infty}^{\infty}\{T_1(\mathbf{x},\lambda_\perp)\eta_x^0\eta_x(t) + T_2(\mathbf{x},\lambda_\perp)\eta_y^0\eta_y(t)\}e^{-z^2/2\lambda_\parallel^2}M_\parallel(z)dz + \langle b_x'^0 T_3(\mathbf{x},\lambda_\perp)\eta_z^{02}\eta_z^2(t)e^{-z^2/2\lambda_\parallel^2}\rangle_\parallel\Bigg\rangle_\perp \times d\eta_x^0 d\eta_y^0 d\eta_z^0 d\mathbf{b}'^0 d\phi^0. \tag{31}$$

The functions T_i contain coupled averages with respect to the perpendicular motion. Following the method outlined above, we use the function $M_\perp(z)$ given in Appendix B. The integrals presented in Appendix C finally yield

$$L_{\mathrm{DCT}}^{(1)} = -\frac{\rho_L^2\beta^2 L_{\lambda_\perp\to\infty}^{(0)}}{v_t^2 b_0^2}\Bigg(\frac{C_\perp(t)[\mathcal{S}_{1a}(t)+3\mathcal{S}_{2a}(t)]}{(1+\langle\xi^2\rangle/\lambda_\perp^2)^5\lambda_\perp^2} - \frac{3\varphi_\perp^2[1-C_\perp(t)]\mathcal{S}_{1b}(t)}{\lambda_\perp^4(1+\langle\xi^2\rangle/\lambda_\perp^2)^{5/2}(1+(\langle\xi^2\rangle+\varphi_\perp^2)/\lambda_\perp^2)^{3/2}} - \frac{15\varphi_\perp^2[1-C_\perp(t)]\mathcal{S}_{2b}(\mathbf{x})}{\lambda_\perp^4(1+\langle\xi^2\rangle/\lambda_\perp^2)^{3/2}(1+(\langle\xi^2\rangle+\varphi_\perp^2)/\lambda_\perp^2)^{5/2}}\Bigg) - \frac{\rho_L^2\beta^2 v_t^2}{b_0^2} \times \frac{\mathcal{S}_3(\mathbf{x})}{\lambda_\parallel^4\sqrt{1+\psi_\parallel/\lambda_\parallel^2}\sqrt{1+\lambda_\parallel^2/(1+\psi_\parallel/\lambda_\parallel^2)}(1+\langle\xi^2\rangle/\lambda_\perp^2)^3}. \tag{32}$$

The functions $\mathcal{S}_i$ are given by

$$\mathcal{S}_i = \int \mathcal{T}_i d\mathbf{b}'^0 d\phi^0 \tag{33}$$

with the $\mathcal{T}$ terms shown in Appendix C. We want to emphasize that $\lim_{\lambda_\perp\to\infty}\mathcal{S}_i(t)=1$ and $\lim_{\lambda_\perp\to 0}\mathcal{S}_i(t)=0$ show the same behavior as in the zeroth order. We have (again) the important relation

$$\lim_{\kappa\to 0} L_{\mathrm{DCT}}^{(1)} = L_{\mathrm{Corrsin}}^{(1)}, \tag{34}$$

verifying the previous result [34] for small Kubo numbers.

IV. RESULTS

In the following we concentrate on the effects caused by large Kubo numbers. Large Kubo numbers correspond to percolative structures of the flux function $\varphi(\mathbf{x},z)$. We will also emphasize finite Larmor radius effects. The conclusions will be drawn from the (numerical) solution of the equation

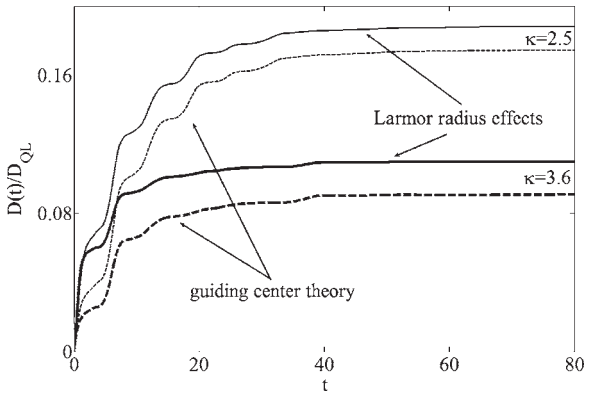

FIG. 1. Solution of Eq. (35). The normalized (by D_{QL}) running diffusion coefficient $D(t)$ is presented in the collisionless case for two different Kubo numbers, $\kappa=2.5$ and $\kappa=3.6$, respectively. A comparison with the predictions of the guiding center theory is shown. The time appears in units of $1/\Omega$, and the stochastic values are $\lambda_{\parallel}=25\rho_L$ and $\beta/b_0=0.1$.

$$\frac{d^2}{dt^2}\langle \delta x^2\rangle = 2\frac{d}{dt}D_{\perp}(t) = L^{(0)}_{\mathrm{DCT}} + L^{(1)}_{\mathrm{DCT}}. \tag{35}$$

The numerical calculation of the DCT structure functions requires an efficient and fast way to solve the integrals for, e.g., φ^0 and $\mathbf{b}^0$. This is a nontrivial task, because for each integration step the decorrelation trajectory has to be recalculated by an additional integration of the nonstochastic three-dimensional Lorentz differential equation system. To perform this task, we use a Monte Carlo integration algorithm which chooses random values for the variable $(\varphi^0, \mathbf{b}^0, \ldots)$ and selects only those with a maximal contribution to the integral.

In Fig. 1 we present the running diffusion coefficient, normalized to the quasilinear coefficient $D_{QL}=v_{\mathrm{th}}\frac{\beta^2}{b_0^2}\lambda_{\parallel}$, in the collisionless case as a function of the time t (in units $1/\Omega$) for two values of the Kubo number. Here, and in the following, the Kubo number is varied by changing $\lambda_{\perp}$, keeping $\lambda_{\parallel}$ as well as β fixed. Thus D_{QL} is constant during the variation and can be used as a proper normalization constant. The guiding center result, that is, the calculation with the zeroth order term $L^{(0)}$ alone, is compared with the complete integration of Eq. (35). The latter contains finite Larmor radius influences. It can be seen that for a larger Kubo number a smaller diffusion rate occurs. Additionally, and probably even more important: In this situation the finite Larmor radius terms lead to higher transport than predicted by the guiding center theory. Obviously guiding center theories underestimate in such cases the diffusion significantly.

Next, we investigate a collisional situation to analyze in what way collisions may compensate the just mentioned amplification effect. Figure 2 shows again the normalized running diffusion coefficient, but now with collisions given by the reduced collisional frequency $\nu/\Omega=0.2$. Note that the Kubo numbers are larger than in Fig. 1. The guiding center prediction is again exceeded by the exact results, for large Kubo numbers. The qualitative result of an amplification of transport at large Kubo numbers is, in principle, not changed by the collisions. Extreme high collisionalities, however,

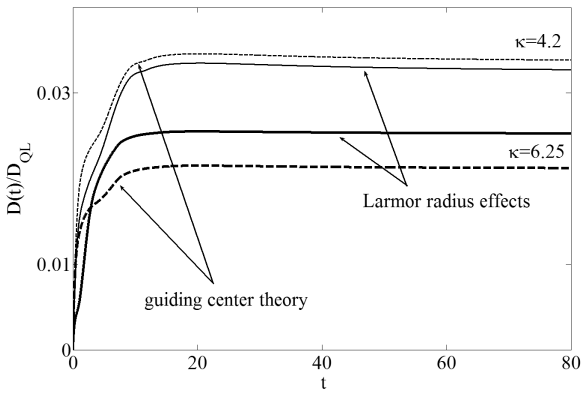

FIG. 2. Same as Fig. 1, but now for a collisional case with $\nu/\Omega=0.2$. Note that the Kubo numbers, $\kappa=4.2$ and $\kappa=6.25$, respectively, are larger than in Fig. 1; the other parameters are unchanged.

may remove any influence of the structure and the typical Corrsin results are recovered. For a fixed value of ν/Ω a certain Kubo number can be found beyond which diffusion is amplified by the Larmor radius effects.

The functional dependence between diffusion and Kubo number is presented in Fig. 3 for the collisionless case. The effect of the finite Larmor radii is shown. For large Kubo numbers, an increase of the diffusion occurs due to the Larmor radius effects. The Larmor radius corrections lead to a significant amplification of the diffusion for very high Kubo numbers. A maximum between $\kappa=100$ and $\kappa=1000$ occurs. Of course, in the limit $\kappa\to\infty$ both rates, the guiding center diffusion and the exact result, decay to zero.

In Fig. 4 we present a typical collisional situation. Two values of the reduced collisional frequency ν/Ω are used. The effect of the increased diffusion for finite Larmor radii prevails.

In order to independently verify our results, we used a Monte Carlo algorithm to simulate the original A-Langevin equation. Figure 5 shows a typical numerical result. The

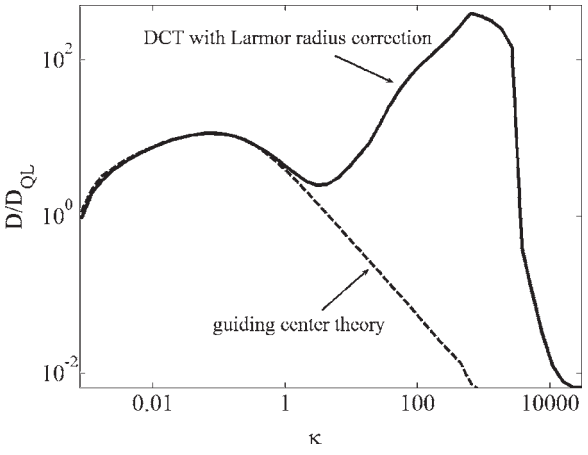

FIG. 3. Normalized diffusion coefficient vs Kubo number, showing amplification caused by finite Larmor radii, for a collisionless situation ($\nu/\Omega=0$). The parameters are $\beta/b_0=0.1$, $\rho_L=2$ measured in units of $v_t/(\Omega b_0)$. The guiding center diffusion was also calculated within the DCT.

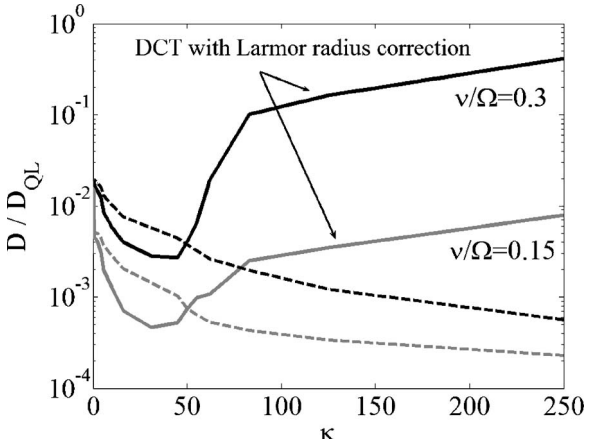

FIG. 4. Normalized diffusion coefficient vs Kubo number for two collisional situations with $\nu/\Omega=0.3$ and $\nu/\Omega=0.15$, respectively. The dashed lines depict the corresponding guiding center results. The parameter values are $\lambda_{\parallel}=25\rho_L$ and $\beta/b_0=0.5$.

mean square displacement is shown as a function of time. The Kubo number is relatively high ($\kappa=125$); collisions are present. When compared to the predictions of the present theory, the agreement is excellent. Guiding center theory underestimates, for the chosen parameters, the diffusion.

V. SUMMARY AND DISCUSSION

In the present paper, for magnetic flux functions with percolative contours the test particle transport was investigated. The calculations started from the so-called *A*-Langevin equations, including stochastic magnetic field components and binary collisions. Using the decorrelation trajectory method (DCT), a relation between the Lagrangian velocity correlation function and the Eulerian magnetic field correlation was derived. There is no restriction on the Kubo number, compared to the Corrsin approximation. Within the Green-Kubo formalism a semianalytical expression for the particle diffusion coefficient was obtained from the Lagrangian velocity correlation function. Finite Larmor radius effects were included. New results for the percolation regime (corresponding to high Kubo numbers) show a significant increase of the transport due to finite Larmor radii. Previous results are found to be limiting cases for small Kubo numbers. An important relation between the decorrelation trajectory method and the Corrsin approximation was found. For different percolative scenarios and collisionalities the diffusion was analyzed, and strong influences of the percolative structures on the transport scaling were found. Direct numerical simulations of the *A*-Langevin equation confirmed the semianalytical predictions.

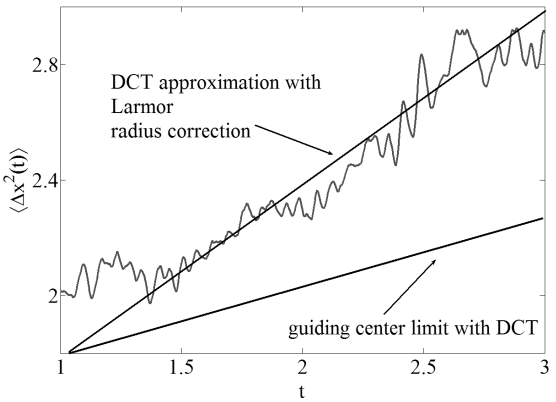

FIG. 5. Monte Carlo simulation of the mean square displacement for a high Kubo number, including collisions and large values of ρ_L, as a function of time t. The parameters are $\kappa=125$, $\nu/\Omega=0.2$, $\beta/b_0=0.5$, $\lambda_{\parallel}=50\rho_L$, and $\lambda_{\perp}=0.2\rho_L$. Straight lines indicate the analytical predictions for the DCT with Larmor radius corrections and the guiding center limit (also calculated with the DCT), respectively.

The general tendency can be understood as follows. We use the analogy [14,23]: ϕ is considered to be a landscape composed of hills and wells. The actual value of ϕ, ϕ^0 can be compared to the level of water filled in this landscape. If we start in the maximum of ϕ, where the landscape is completely flooded and decrease the water level ϕ^0, the number of hills increases together with their sizes. At certain levels the coalescence of different hills is observed, because ϕ^0 passes the hyperbolic points of the percolation map. Whenever such a coalescence takes place, the area and the contour line of the hill suddenly increase, and with it the area along which a field line is allowed to travel. High Kubo numbers represent ϕ regimes with distinct extremas, hence many hills. The particle diffusion is essentially reduced because a certain number of particles remain in trapped states with their field lines. Such a particle contributes to the diffusion process again, if it is dislocated to a lower ϕ^0 value by a collision. Higher collisionality therefore reduces the trapping effect. In a similar way, finite Larmor radii work against trapping. On the other hand, a situation with less hills or many united hills, i.e., a smooth landscape, is realized for small Kubo numbers. In such regimes trapping does not play an important role and can be neglected.

ACKNOWLEDGMENTS

This work was performed under the auspices of the SFB 591. Interesting discussions with Sadrilla Abdullaev, Reinhard Schlickeiser, and Andreas Wingen are gratefully acknowledged.

APPENDIX A: STOCHASTIC PROPERTIES OF THE FLUX FUNCTION

The flux function is a stochastic object. Its Eulerian correlation function is defined as

$$A(\mathbf{x},z)=\langle\phi(\mathbf{0},0)\phi(\mathbf{x},z)\rangle=\beta^2\lambda_{\perp}^2\exp[-\Theta(\mathbf{x},z)]. \quad \text{(A1)}$$

We assume a Gaussian with

$$\Theta(\mathbf{x},z)\equiv\frac{x^2+y^2}{2\lambda_{\perp}^2}+\frac{z^2}{2\lambda_{\parallel}^2}. \quad \text{(A2)}$$

In the main part, we derived the Lagrangian correlator from the Eulerian correlator of the **b** field. The latter can be recovered from the present formulation via

$$\boldsymbol{\mathcal{E}} = \langle \mathbf{b}(0) \otimes \mathbf{b}(x) \rangle = \langle (\boldsymbol{\nabla} \times \phi \mathbf{e}_z) \otimes (\boldsymbol{\nabla} \times \phi \mathbf{e}_z) \rangle = \begin{pmatrix} -\partial_{yy}A & \partial_{yx}A \\ \partial_{xy}A & -\partial_{xx}A \end{pmatrix} \equiv \begin{pmatrix} \mathcal{E}_{xx} & \mathcal{E}_{xy} \\ \mathcal{E}_{yx} & \mathcal{E}_{yy} \end{pmatrix}. \tag{A3}$$

The off-diagonal elements are the cross correlations. They are given by

$$\mathcal{E}_{x\phi} = -\mathcal{E}_{\phi x} = \partial_y A, \quad \mathcal{E}_{y\phi} = -\mathcal{E}_{\phi x} = -\partial_x A. \tag{A4}$$

Correlations of the derivatives with respect to the time t are given by

$$\bar{\mathcal{E}}_{ii} = \langle b_i'(t_1) b_i'(t_2) \rangle = \frac{d^2}{dt_1 dt_2} \langle b_x(t_1) b_x(t_2) \rangle = \begin{pmatrix} -\partial_{yy}\bar{A} & \partial_{yx}\bar{A} \\ \partial_{xy}\bar{A} & -\partial_{xx}\bar{A} \end{pmatrix}, \tag{A5}$$

where we have defined

$$\begin{aligned} \bar{A} &= \left(\frac{d^2}{dt_1 dt_2} A(\mathbf{x}(t_1) - \mathbf{x}(t_2), z(t_1) - z(t_2)) \right)_{t_1 = t, t_2 = 0} \\ &= \left[\left(\beta^2 - \frac{x^2\beta^2}{\lambda_\perp^2} \right) \eta_x^0 \eta_x(t) + \left(\beta^2 - \frac{y^2\beta^2}{\lambda_\perp^2} \right) \eta_y^0 \eta_y(t) \right. \\ &\quad \left. + \left(\frac{\beta^2\lambda_\perp^2}{\lambda_\parallel^2} - \frac{z^2\beta^2\lambda_\perp^2}{\lambda_\parallel^4} \right) \eta_z^0 \eta_z(t) \right] \exp[-\Theta(\mathbf{x}, z)]. \end{aligned} \tag{A6}$$

With the prescription (A6) the correlation functions can be obtained from Eq. (A5). All cross correlations of the type $\eta_x \eta_y$ are neglected since they vanish when the correlators are averaged. The same reason causes $\mathcal{E}_{\phi b'} = \langle \phi(0) b_x'(t) \rangle = 0$ because only single η_i elements appear.

APPENDIX B: COUPLED AVERAGE PROBABILITIES

Here we focus on the combined averages needed in the DCT equations. The subensemble averages are obtained by accounting for the conditional averages in the following way:

$$\begin{aligned} &\langle\langle \eta_\parallel(t) \mathbf{b}[\mathbf{x}(t), z(t), t] \rangle_S \rangle_\perp \\ &= \int_{-\infty}^{\infty} \int_{-\infty}^{\infty} \int_{-\infty}^{\infty} \frac{\langle \eta_z(t) \delta(z - z(t)) \delta(\eta_z^0 - \eta_z(0)) \rangle_\parallel}{P(\eta_0)} \\ &\quad \times \frac{1}{\langle \delta(\phi^0 - \phi(\mathbf{0})) \delta(\mathbf{b}^0 - \mathbf{b}(\mathbf{0})) \rangle_S} \\ &\quad \times \langle\langle \delta(b - b(\mathbf{x} + \boldsymbol{\xi}, z, t)) \delta(\phi^0 - \phi(\mathbf{0})) \delta(\mathbf{b}^0 - \mathbf{b}(\mathbf{0})) \rangle_S \\ &\quad \times \delta(\xi_x - \xi_x(t)) \delta(\xi_y - \xi_y(t)) \rangle_\perp \langle \delta(\phi^0 - \phi(\mathbf{0})) \\ &\quad \times \delta(\mathbf{b}^0 - \mathbf{b}(\mathbf{0})) \rangle_S d\xi_x d\xi_y dz, \end{aligned} \tag{B1}$$

and

$$\begin{aligned} &\langle\langle \eta_\parallel(t) \mathbf{b}'[\mathbf{x}(t), z(t), t] \rangle_S \rangle_\perp \\ &= \int_{-\infty}^{\infty} \int_{-\infty}^{\infty} \int_{-\infty}^{\infty} \frac{\langle \eta_z(t) \delta(z - z(t)) \delta(\eta_z^0 - \eta_z(0)) \rangle_\parallel}{P(\eta_0)} \\ &\quad \times \frac{1}{\langle \delta(\mathbf{b}^0 - \mathbf{b}(\mathbf{0})) \rangle_S} \\ &\quad \times \langle\langle \delta(b' - b'(\mathbf{x} + \boldsymbol{\xi}, z, t)) \delta(\mathbf{b}' 0 - \mathbf{b}(\mathbf{0})) \rangle_S \\ &\quad \times \delta(\xi_x - \xi_x(t)) \delta(\xi_y - \xi_y(t)) \rangle_\perp d\xi_x d\xi_y dz. \end{aligned} \tag{B2}$$

The averaging is performed as follows: (i) The first conditional average term in both expressions depend on η_z. They take the parallel motion into account. The latter appears within the b field as well as in the velocity correlator itself. Here, we are not allowed to make a stochastic independence assumption for these terms, as is being done in the Corrsin approximation. (ii) Perpendicular averaging is performed by applying two δ functions for ξ_x and ξ_y. Unfortunately the procedure becomes more complicated for the average with derivative terms. Because of the η_x and η_y product terms we need the same procedure as for the parallel motion.

Next, we determine the conditional average for the parallel motion,

$$M_\parallel(z) \equiv \frac{\langle \eta_z(t) \delta(z - z(t)) \delta(\eta_z^0 - \eta_z(0)) \rangle_\parallel}{\langle \delta(\eta_z^0 - \eta_z(0)) \rangle_\parallel}. \tag{B3}$$

The Fourier representation of the δ functions helps to rewrite the stochastic data in the form of exponential functions and leads to the integrations,

$$\begin{aligned} M_\parallel(z) = \frac{1}{2\pi P(\eta^0)} \int \int \exp[-ikz - iq\eta_z^0] \\ \times \langle \eta_z(t) \exp[ikz(t) + iq\eta_z(0)] \rangle_\parallel dk dq. \end{aligned} \tag{B4}$$

To simplify the last expression, we define the function

$$\langle H_\parallel \rangle_\parallel \equiv \langle \exp[a\eta_z(t) + ikz(t) + iq\eta_z(0)] \rangle_\parallel, \tag{B5}$$

which is related to the unknown average by

$$\langle \eta_z(t) \exp[ikz(t) + iq\eta_z(0)] \rangle_\parallel = \left[\left\langle \frac{\partial}{\partial a} H \right\rangle_\parallel \right]_{a=0}. \tag{B6}$$

In this form, the parallel average is applied to H by the standard cumulant expansion,

$$\begin{aligned} \langle H_\parallel \rangle_\parallel = \exp\left(-\frac{a^2}{2} \langle \eta_z(t) \eta_z(t) \rangle_\parallel - \frac{k^2}{2} \langle z^2(t) \rangle_\parallel - \frac{q^2}{2} \langle \eta_z(0) \eta_z(0) \rangle_\parallel \right. \\ \left. + iaq \langle \eta_z(0) \eta_z(t) \rangle_\parallel - kq \langle z(t) \eta_z(0) \rangle_\parallel + iak \langle z(t) \eta_z(t) \rangle_\parallel \right). \end{aligned} \tag{B7}$$

Here, the well-known stochastic properties of η_z can be used,

$$\begin{aligned} &\langle \eta_z(t) \eta_z(t) \rangle_\parallel = \langle \eta_z(0) \eta_z(0) \rangle_\parallel = 1, \\ &\langle \eta_z(t_1) \eta_z(t_2) \rangle_\parallel = \chi_\parallel \nu e^{-\nu |t_1 - t_2|} \equiv C_\parallel(t), \\ &\langle z(t) \eta_z(t) \rangle_\parallel = \langle z(t) \eta_z(0) \rangle_\parallel = \varphi_\parallel(t), \\ &\langle z^2(t) \rangle_\parallel = \psi_\parallel(t). \end{aligned} \tag{B8}$$

The average $H_\parallel$ simplifies to

$$\langle H_{\parallel}\rangle_{\parallel} = \exp\left(-\frac{a^2}{2} - \frac{k^2}{2}\psi_{\parallel}(t) - \frac{q^2}{2} + iaqC_{\parallel}(t) - kq\varphi_{\parallel}(t) + iak\varphi_{\parallel}(t)\right), \tag{B9}$$

and the derivative at $a=0$ is

$$\frac{\partial}{\partial a}\langle H_{\parallel}\rangle_{\parallel a=0} = [iqC_{\parallel}(t) + ik\varphi_{\parallel}(t)] \times \exp\left(-\frac{q^2}{2} - \frac{k^2}{2}\psi_{\parallel}(t) - kq\varphi_{\parallel}(t)\right). \tag{B10}$$

To find $M_{\parallel}$, we use the definition of $H_{\parallel}$ in the expression for $M_{\parallel}$:

$$M_{\parallel}(z) = \frac{1}{2\pi P(\eta^0)}\int\int [iqC_{\parallel}(t) + ik\varphi_{\parallel}(t)]\exp\left(-\frac{q^2}{2} - \frac{k^2}{2}\psi_{\parallel}(t) - kq\varphi_{\parallel}(t)\right)\exp[-ikz - iq\eta_z^0]dkdq. \tag{B11}$$

Performing the integration over q leads to

$$M_{\parallel}(z) = \frac{1}{\sqrt{2\pi}P(\eta_z^0)}\int [\eta_z^0 C_{\parallel}(t) - ik(R-1)\varphi_{\parallel}(t)] \times \exp\left(-\frac{1}{2}[\eta_z^0 - ik\varphi_{\parallel}(t)]^2 - ikz - \frac{k^2}{2}\psi_{\parallel}(t)\right)dk. \tag{B12}$$

Finally, the integration over k yields

$$M_{\parallel}(z) = \left(\frac{\eta_z^0 C_{\parallel}(t)}{[\psi_{\parallel}(t) - \varphi_{\parallel}^2(t)]^{1/2}} + \frac{\varphi_{\parallel}(t)(1 - C_{\parallel}(t))[z - \eta_z^0\varphi_{\parallel}(t)]}{[\psi_{\parallel}(t) - \varphi_{\parallel}^2(t)]^{3/2}}\right) \times \exp\left(\frac{\eta_z^{02}}{2} - \frac{z^2 + \psi_{\parallel}(t)\eta_z^{02} - 2z\eta_z^2\varphi_{\parallel}(t)}{2[\psi_{\parallel}(t) - \varphi_{\parallel}^2(t)]}\right), \tag{B13}$$

and after some algebraic manipulations we find

$$M_{\parallel}(z) = \left(\frac{\eta_z^0 C_{\parallel}(t)}{[\psi_{\parallel}(t) - \varphi_{\parallel}^2(t)]^{1/2}} + \frac{\varphi_{\parallel}(t)[1 - C_{\parallel}(t)][z - \eta_z^0\varphi_{\parallel}(t)]}{[\psi_{\parallel}(t) - \varphi_{\parallel}^2(t)]^{3/2}}\right) \times \exp\left(-\frac{[z - \eta_z^0\varphi_{\parallel}(t)]^2}{2[\psi_{\parallel}(t) - \varphi_{\parallel}^2(t)]}\right). \tag{B14}$$

The last result can be expressed in terms of a probability distribution $P(z)$,

$$M_{\parallel}(z) = \left\{\eta_z^0 C_{\parallel}(t) - \frac{\eta_z^0\varphi_{\parallel}^2(t)}{[\psi_{\parallel}(t) - \varphi_{\parallel}^2(t)]}\left[1 - C_{\parallel}(t)\frac{\partial}{\partial z}\right]\right\}P_{\parallel}(z), \tag{B15}$$

using the subensemble average of the position $\langle z(t)\rangle = \eta_z^0\varphi_{|}(t)$ and

$$P(z) = \frac{1}{\sqrt{2\pi[\psi_{\parallel}(t) - \varphi_{\parallel}^2(t)]}}\exp\left(-\frac{[z - \langle z(t)\rangle_S]^2}{2[\psi_{\parallel}(t) - \varphi_{\parallel}^2(t)]}\right). \tag{B16}$$

Such an expression can also be found in Ref. [28] derived for a DCT approximation within the context of the V-Langevin equations.

The conditional average of the perpendicular motion is found analogously,

$$M_{\perp}(\xi_x) \equiv \frac{\langle \eta_x(t)\,\delta(\xi_x - \xi_x(t))\,\delta(\eta_x^0 - \eta_x(0))\rangle_{\perp}}{\langle \delta(\eta_x^0 - \eta_x(0))\rangle_{\parallel}}. \tag{B17}$$

Due to the symmetry the same arguments hold for $M_{\perp}(\xi_y)$. Designating

$$\langle \eta_x(t)\,\eta_x(t)\rangle_{\perp} = \langle \eta_x(0)\,\eta_x(0)\rangle_{\perp} = 1,$$

$$\langle \eta_x(t_1)\,\eta_x(t_2)\rangle_{\perp} = \chi_{\perp}\nu e^{-\nu|t_1 - t_2|} \equiv C_{\perp}(t), \tag{B18}$$

and using the data from the classical transport,

$$\langle \xi_x(t)\,\eta_x(t)\rangle_{\perp} = \langle \xi_x(t)\,\eta_x(0)\rangle_{\perp} = \varphi_{\perp}(t), \tag{B19}$$

we find

$$M_{\perp}(\xi_x) = \left\{\eta_x^0 C_{\perp}(t) - \varphi_{\perp}(t)[1 - C_{\perp}(t)]\frac{d}{d\xi_x}\right\}P_{\perp}(\xi_x). \tag{B20}$$

APPENDIX C: THE $\mathcal{T}_i$ FUNCTIONS AND THE STRUCTURE INTEGRALS $\mathcal{S}_i$

The $\mathcal{T}_i$ terms can be calculated analytically. The results of the integration are the following:

$$\mathcal{T}_{1a}(\mathbf{x}) = \frac{1}{(1 + \langle\xi^2\rangle/\lambda_{\perp}^2)^3\lambda_{\perp}^4} \times [(\lambda_{\perp}^2 + \langle\xi^2\rangle - x^2)(\lambda_{\perp}^2 + \langle\xi^2\rangle - y^2)b_x'^0 + xy(3\lambda_{\perp}^2 + 3\langle\xi^2\rangle - x^2)b_y'^0] \times \exp\left(-\frac{x^2 + y^2}{2(\langle\xi^2\rangle + \lambda_{\perp}^2)}\right), \tag{C1}$$

$$\mathcal{T}_{1b}(\mathbf{x}) = \frac{1}{3[1 + (\langle\xi^2\rangle + \varphi_{\perp}^2)/\lambda_{\perp}^2]^4\lambda_{\perp}^8}\{(\langle\xi^2\rangle - y^2 + \lambda_{\perp}^2) \times b_x'^0(\langle\xi^2\rangle + \lambda_{\perp}^2 + \varphi_{\perp}^2)[3\langle\xi^2\rangle^2 - 6\langle\xi^2\rangle x^2 + x^4 + 6(\langle\xi^2\rangle - x^2)\lambda_{\perp}^2 + 3\lambda_{\perp}^4 + 6(\langle\xi^2\rangle - x^2 + \lambda_{\perp}^2)\varphi_{\perp}^2 + 3\varphi_{\perp}^4] + xy(\langle\xi^2\rangle + \lambda_{\perp}^2) \times b_y'^0[15\langle\xi^2\rangle^2 + x^4 - 10x^2\lambda_{\perp}^2 + 15\lambda_{\perp}^4 - 10\langle\xi^2\rangle \times (x^2 - 3\lambda_{\perp}^2) + 5\varphi_{\perp}^2(6\langle\xi^2\rangle - 2x^2 + 6\lambda_{\perp}^2 + 3\varphi_{\perp}^2)]\} \times \exp\left(-\frac{x^2}{2(\langle\xi^2\rangle + \lambda_{\perp}^2 + \varphi_{\perp}^2)} - \frac{y^2}{2(\langle\xi^2\rangle + \lambda_{\perp}^2)}\right). \tag{C2}$$

$$\mathcal{T}_{2a}(\mathbf{x}) = \frac{1}{3(1+\langle\xi^2\rangle/\lambda_\perp^2)^2\lambda_\perp^4}\{[3\langle\xi^2\rangle^2 + y^4 - 6y^2\lambda_\perp^2 + 3\lambda_\perp^4 - 6\langle\xi^2\rangle(y^2-\lambda_\perp^2)]b_x'^0 + xy(3\langle\xi^2\rangle - y^2 + 3\lambda_\perp^2)b_y'^0\} \times \exp\left(-\frac{x^2+y^2}{2(\langle\xi^2\rangle+\lambda_\perp^2)}\right), \quad \text{(C3)}$$

$$\mathcal{T}_{2b}(\mathbf{x}) = -\frac{1}{15[1+(\langle\xi^2\rangle+\varphi_\perp^2)/\lambda_\perp^2]^4\lambda_\perp^8} \times(-xyb_y'^0(\langle\xi^2\rangle+\lambda_\perp^2+\varphi_\perp^2) \times[15\langle\xi^2\rangle^2 + y^4 - 10y^2\lambda_\perp^2 + 15\lambda_\perp^4 - 10\langle\xi^2\rangle(y^2-3\lambda_\perp^2) + 5\varphi_\perp^2(6\langle\xi^2\rangle - 2y^2 + 6\lambda_\perp^2 + 3\varphi_\perp^2)] - (\langle\xi^2\rangle+\lambda_\perp^2)b_x'^0\{15\langle\xi^2\rangle^3 - 45\langle\xi^2\rangle^2y^2 + 15\langle\xi^2\rangle y^4 - y^6 + 15(3\langle\xi^2\rangle^2 - 6\langle\xi^2\rangle y^2 + y^4)\lambda_\perp^2 + 45(\langle\xi^2\rangle - y^2)\lambda_\perp^4 + 15\lambda_\perp^6 + 15\varphi_\perp^2[3\langle\xi^2\rangle^2 - 6\langle\xi^2\rangle y^2 + y^4 + 6(\langle\xi^2\rangle - y^2)\lambda_\perp^2 + 3\lambda_\perp^4 + 3(\langle\xi^2\rangle - y^2 + \lambda_\perp^2)\varphi_\perp^2 + \varphi_\perp^4]\}) \times \exp\left(-\frac{x^2}{2(\langle\xi^2\rangle+\lambda_\perp^2)} - \frac{y^2}{2(\langle\xi^2\rangle+\lambda_\perp^2+\varphi_\perp^2)}\right), \quad \text{(C4)}$$

$$\mathcal{T}_3(\mathbf{x}) = \frac{1}{\lambda_\perp^2}[(\langle z^2\rangle - y^2 + \lambda_\perp^2)b_x'^0 + xyb_y'^0] \times \exp\left(-\frac{x^2+y^2}{2(\langle\xi^2\rangle+\lambda_\perp^2)}\right). \quad \text{(C5)}$$

[1] R. Balescu, *Aspects of Anomalous Transport in Plasmas* (Institute of Physics Publishing, Bristol, 2005).
[2] R. Balescu, *Transport Processes in Plasmas: 2. Neoclassical Transport Theory* (North-Holland, Amsterdam, 1988).
[3] Y. Elskens and D. Escande, *Microscopic Dynamics of Plasmas and Chaos* (Institute of Physics Publishing, Bristol, 2003).
[4] T. E. Evans *et al.*, Phys. Rev. Lett. **92**, 235003 (2004).
[5] Y. Liang *et al.*, Phys. Rev. Lett. **94**, 105003 (2005).
[6] K. H. Finken, S. S. Abdullaev, M. Jakubowski, R. C. Wolf, G. Matsunaga, U. Samm, K. H. Spatschek, M. Tokar, and B. Unterberg, Phys. Rev. Lett. **94**, 015003 (2005).
[7] M. W. Jakubowski *et al.*, Phys. Rev. Lett. **96**, 035004 (2006).
[8] S. S. Abdullaev, *Construction of Mappings for Hamiltonian Systems and Their Applications* (Springer, Berlin, 2006).
[9] S. S. Abdullaev, A. Wingen, and K. H. Spatschek, Phys. Plasmas **713**, 042509 (2006).
[10] R. Kubo, J. Math. Phys. **4**, 174 (1963).
[11] R. Balescu, *Statistical Dynamics, Matter out of Equilibrium* (Imperial College Press, London, 2000).
[12] J. R. Jokipii, Astrophys. J. **183**, 1029 (1973).
[13] A. B. Rechester and M. N. Rosenbluth, Phys. Rev. Lett. **40**, 38 (1978).
[14] D. Ruffolo, W. H. Matthaeus, and P. Chuychai, Astrophys. J. **614**, 420 (2004).
[15] P. Chuychai, D. Ruffolo, W. H. Matthaeus, and G. Rowlands, Astrophys. J. Lett. **633**, L49 (2005).
[16] G. Qin, W. H. Matthaeus, and J. W. Bieber, Astrophys. J. Lett. **578**, L117 (2002).
[17] W. H. Matthaeus, G. Qin, J. W. Bieber, and G. P. Zank, Astrophys. J. Lett. **590**, L000 (2003).
[18] F. Casse, M. Lemoine, and G. Pelletier, Phys. Rev. D **65**, 023002 (2001).
[19] D. Ruffolo, W. H. Matthaeus, and P. Chuychai, Astrophys. J. Lett. **597**, L169 (2003).
[20] A. Shalchi, J. W. Bieber, W. H. Matthaeus, and R. Schlickeiser, Astrophys. J. **642**, 230 (2006).
[21] J. Jokipii, Astrophys. J. **146**, 480 (1966).
[22] B. B. Kadomtsev and O. P. Pogutse, in *Plasma Physics and Controlled Nuclear Fusion Research, Proceedings of the 7th International Conference* (1978), Vol. 1, p. 549.
[23] M. B. Isichenko, Plasma Phys. Controlled Fusion **33**, 795 (1991).
[24] M. B. Isichenko, Plasma Phys. Controlled Fusion **33**, 809 (1991).
[25] M. B. Isichenko, Rev. Mod. Phys. **64**, 961 (1992).
[26] M. Vlad, F. Spineanu, J. H. Misguich, and R. Balescu, Phys. Rev. E **58**, 7359 (1998).
[27] M. Vlad, F. Spineanu, J. H. Misguich, and R. Balescu, Phys. Rev. E **63**, 066304 (2001).
[28] M. Vlad, F. Spineanu, J. H. Misguich, and R. Balescu, Phys. Rev. E **67**, 026406 (2003).
[29] M. Vlad and F. Spineanu, Plasma Phys. Controlled Fusion **47**, 281 (2005).
[30] J.-D. Reuss and J. H. Misguich, Phys. Rev. E **54**, 1857 (1996).
[31] S. Corrsin, in *Atmospheric Diffusion and Air Pollution*, edited by F. N. Frenkiel and P. A. Sheppard (Academic, New York, 1990), p. 161.
[32] E. Vanden-Eijnden and R. Balescu, Phys. Plasmas **3**, 874 (1996).
[33] M. Vlad, F. Spineanu, J. H. Misguich, J.-D. Reuss, R. Balescu, K. Itoh, and S.-I. Itoh, Plasma Phys. Controlled Fusion **46**, 1051 (2004).
[34] M. Neuer and K. H. Spatschek, Phys. Rev. E **73**, 026404 (2006).